# Printing Non-Euclidean Solids

Giuseppe Zurlo[1,*] and Lev Truskinovsky[2,†]
[1]School of Mathematics, Statistics and Applied Mathematics, NUI Galway, University Road, Galway, Ireland
[2]PMMH, CNRS—UMR 7636 PSL-ESPCI, 10 Rue Vauquelin, 75005 Paris, France
(Received 8 March 2017; published 26 July 2017)

Geometrically frustrated solids with a non-Euclidean reference metric are ubiquitous in biology and are becoming increasingly relevant in technological applications. Often they acquire a targeted configuration of incompatibility through the surface accretion of mass as in tree growth or dam construction. We use the mechanics of incompatible surface growth to show that geometrical frustration developing during deposition can be fine-tuned to ensure a particular behavior of the system in physiological (or working) conditions. As an illustration, we obtain an explicit 3D printing protocol for arteries, which guarantees stress uniformity under inhomogeneous loading, and for explosive plants, allowing a complete release of residual elastic energy with a single cut. Interestingly, in both cases reaching the physiological target requires the incompatibility to have a topological (global) component.

DOI: 10.1103/PhysRevLett.119.048001

Externally unloaded elastic solids can be still endogenously prestressed by distributed self-equilibrated force couples. In living organisms such preconditioning is a way of achieving specific targets in physiological regimes [1]; for instance, vegetable leafs require residual stresses to open [2] while arteries need a preload to ensure transmural uniformity of the hoop stress [3]. Residual stresses are equally important in engineering applications, where preloading is used either for reinforcement or to delay the onset of failure [4,5]. Furthermore, challenging new applications, like the design of programmable biomimetic materials, depend crucially on our ability to create complex patterns of residual stresses [6–10].

In this Letter we address the question of how a particular distribution of residual stresses can be produced in a solid as a result of the surface accretion of mass, a central process in both natural growth and 3D printing.

The source of residual stresses in elastic solids is the incompatibility of the reference configuration, which prevents its isometric embedding into the Euclidean space. A reference (natural) state is characterized by a metric tensor and in Euclidean solids this metric is flat [11,12]. In "non-Euclidean solids," a term apparently coined by Poincaré [13], the reference metric is curved, and the associated geometrical frustration manifests itself through residual stresses [14].

A reference curvature can be "embedded" into a solid by using rather well understood techniques of differential swelling, inhomogeneous thermal expansion, bulk growth, and remodeling [1,15–18]. Geometrical frustration can also emerge as a result of surface accretion, as in tree growth, roll winding, and dam construction [19–23]. In the case of surface growth, the relation between the physics of deposition and the resulting incompatibility is implicit and it is not clear which accretion protocol leads to a desired distribution of residual stresses.

Surface growth is often modeled in a holonomic format of elastically coherent phase transitions, which take place without the generation of incompatibility [24,25]. A more general, nonholonomic approach should allow for the incompatibility to be acquired at the moment of the creation of a new continuum of particles, see for instance Refs. [26–28]. In this Letter we consider a general inverse problem of this type and view the deposition stress as a tensorial control parameter. We find an explicit link between the implemented deposition strategy and the resulting incompatibility. The obtained relations not only reveal the mechanisms of biological adaptation associated with surface growth, but can also guide the additive manufacturing of programmable metamaterials.

To illustrate the general theory, we study in detail the process of artificial 3D printing of arteries. Presently, the circumferential wrapping of sheets of living cells is used to reproduce their natural layered structure [29–31]. However, in physiological conditions the resulting transmural stress distribution is far from realistic [32,33]. Instead, our approach allows one to reach the target physiological state precisely, and we show that the proposed strategy is compatible with available manufacturing technologies. As another illustration, we design a growth protocol ensuring that a single cut in a hollow cylinder results in a complete release of the residually stored elastic energy. This prototypical problem is relevant for the understanding of explosive seed dispersal and other functions of plant actuators [34–36]. Quite remarkably, we find that in both biological examples the crucial role is played by a global contribution to incompatibility, usually associated with topological defects in crystals (disclinations) [37].

Consider a body $\mathcal{B}_p$ that in physiological (or working) conditions is subjected to tractions $\mathbf{s}_p$ applied on its boundary $\omega_p$. The symmetric physiological stress field $\boldsymbol{\sigma}_p(\boldsymbol{x})$ must satisfy the equilibrium conditions

 

$$\mathrm{div}\boldsymbol{\sigma}_p = \mathbf{0} \quad \text{in} \quad \mathcal{B}_p, \qquad \boldsymbol{\sigma}_p \boldsymbol{n} = \mathbf{s}_p \quad \text{on} \quad \omega_p, \quad (1)$$

where $\boldsymbol{n}$ is the outward normal. Since the generic problem of this kind is not statically determinate, in the absence of additional equations the stress remains underdetermined. If the deformation is Euclidean the problem can be closed by supplementing Eq. (1) with relations expressing the stress in terms of the gradient of the displacement. This leads to a distribution of stresses that can be altered only by changing the shape of the body or by varying the elastic properties of the material. An alternative way to control the stress state of the body and its deformed shape, apparently favored by biological systems, is to give up the compatibility and employ inelastic deformations.

Suppose (for simplicity) that Hooke's law still holds for incremental deformations and define the (linear) elastic strain $\boldsymbol{\epsilon}_p = \mathbb{C}^{-1}\boldsymbol{\sigma}_p$, where $\mathbb{C}$ is the elasticity tensor. The signature of the non-Euclidean character of the stress is the nonzero incompatibility $\boldsymbol{\eta}_p = \mathrm{curlcurl}\boldsymbol{\epsilon}_p$, the linear counterpart of the reference Riemann curvature, which satisfies the Bianchi identities $\mathrm{div}\boldsymbol{\eta}_p = \mathbf{0}$. If a target incompatibility $\boldsymbol{\eta}_p$ is prescribed, its three independent components remain unconstrained by Eq. (1) and can be used to "engineer" a particular physiological state of stress. Embedding a strain incompatibility can be viewed as a way of "programming" the material, making it "information rich" [38,39]. The ultimate performance of such materials will of course also depend on the loads and the shape of the body, e.g., Ref. [10], while the targets may be as diverse as microscopic stress channeling and macroscopic multistability.

Note that $\boldsymbol{\eta}_p$ should be understood in the sense of distributions [40], because the target incompatibility may contain both diffuse and singular contributions. Furthermore, singular defect lines may have a global effect if they carry topological charges characterized by the nonzero Burgers $\mathbf{B}_p(\boldsymbol{x}_0) = \lim_{h\to 0}\int_{D_h} \boldsymbol{y}\times\boldsymbol{\eta}_p^{\mathsf{T}}\boldsymbol{n}da$ and Frank $\boldsymbol{\Omega}_p(\boldsymbol{x}_0) = \lim_{h\to 0}\int_{D_h}\boldsymbol{\eta}_p^{\mathsf{T}}\boldsymbol{n}da$ vectors [16,41–43], where $\boldsymbol{y}$ is the position vector of points of an asymptotically shrinking oriented disk $D_h$ of diameter $h$, enclosing the singular point $\boldsymbol{x}_o$ [47]. Since the associated residual stresses cannot be removed by cutting singular lines out of the body, in non–simply connected bodies such topological charges may be located outside the domain $\mathcal{B}_p$.

To model a nonholonomically growing body we introduce a sequence of (incremental) configurations $\mathcal{B}(t)$. The timelike parameter $t$ changes in the interval $(t_i, t_f)$, denoting the beginning and the end of the accretion process. In particular, $\mathcal{B}(t_f) = \mathcal{B}_p$. We denote by $\tau(\boldsymbol{x})$ the instant when the accreting surface $\omega(t)$, whose evolution is assumed to be known, passes through a (Lagrangian) point $\boldsymbol{x}$.

Equilibrium must hold at each stage of growth, so in the absence of body forces (a simplifying assumption) we must have $\mathrm{div}\boldsymbol{\sigma} = \mathbf{0}$ in $\mathcal{B}(t)$. Consider surface growth as a moving boundary problem. Suppose that on the advancing (nonmaterial) surface $\omega(t)$

$$[\![\boldsymbol{\sigma}]\!] \equiv \boldsymbol{\sigma}(\boldsymbol{x},t) - \mathring{\boldsymbol{\sigma}}(\boldsymbol{x}) = 0, \quad (2)$$

where the deposition stress $\mathring{\boldsymbol{\sigma}}(\boldsymbol{x})$ is prescribed by the attachment protocol. This tensor can be decomposed into a sum of two (rank-2) contributions: $\mathring{\boldsymbol{\sigma}}(\boldsymbol{x}) = \boldsymbol{p}(\boldsymbol{x}) + \mathring{\boldsymbol{\sigma}}_a(\boldsymbol{x})$, see Fig. 1. While the "passive" contribution $\boldsymbol{p} = \mathbf{s}\otimes\boldsymbol{n} + \boldsymbol{n}\otimes\mathbf{s} - (\mathbf{s}\cdot\boldsymbol{n})\boldsymbol{n}\otimes\boldsymbol{n}$ is fully defined by the applied tractions $\mathbf{s} = \boldsymbol{\sigma}\boldsymbol{n}$, the "active" surface stress $\mathring{\boldsymbol{\sigma}}_a$, satisfying $\mathring{\boldsymbol{\sigma}}_a\boldsymbol{n} = \mathring{\boldsymbol{\sigma}}_a^{\mathsf{T}}\boldsymbol{n} = \mathbf{0}$, carries three independent degrees of freedom that can be used to "implant incompatibility" in the upcoming layers.

The breakdown of $\mathring{\boldsymbol{\sigma}}$ into active and passive contributions is somewhat arbitrary, because in natural and technological conditions the three components of $\boldsymbol{p}$ may also play the role of active agents. In some cases the implied freedom disappears: during coherent structural transformations the whole stress $\mathring{\boldsymbol{\sigma}}$ is determined by the evolution laws of the interface [25,48]; for solidification, it is natural to assume that the active term adjusts to ensure that $\mathring{\boldsymbol{\sigma}}$ is hydrostatic [49]; for surface growth in plants and in some additive manufacturing processes, the adhering layer can be treated as a prestressed elastic membrane, whose state of deformation is controlled by the requirement of equilibrium under suitable anchoring and adhesion conditions [50,51]. Here, we neglect the potential constraints imposed by the deposition mechanism and we treat the independent components of $\mathring{\boldsymbol{\sigma}}_a$ as free control parameters.

At $t \geq \tau(\boldsymbol{x})$ the stress tensor in the growing body can be written as $\boldsymbol{\sigma}(\boldsymbol{x},t) = \mathring{\boldsymbol{\sigma}}(\boldsymbol{x}) + \int_{\tau(\boldsymbol{x})}^{t}\dot{\boldsymbol{\sigma}}(\boldsymbol{x},s)ds$ and the incremental equilibrium requires that $\mathrm{div}\dot{\boldsymbol{\sigma}} = \mathbf{0}$ in $\mathcal{B}(t)$. To obtain the boundary conditions for this equation we note that in view of Eq. (2) $[\![\nabla\boldsymbol{\sigma}]\!] = \boldsymbol{\lambda}\otimes\boldsymbol{N}$, where both the gradient and the normal are in 4D (space-time) [52], while $\boldsymbol{\lambda}$ is a second order tensor in 3D (space) [53]. One consequence of such Hadamard condition is that $[\![\dot{\boldsymbol{\sigma}}]\!]\boldsymbol{n} = -V[\![\mathrm{div}\boldsymbol{\sigma}]\!]$, where $V = |\nabla\tau|^{-1}$ is the normal velocity of $\omega(t)$. Specialization to our case gives

$$\dot{\boldsymbol{\sigma}}(\boldsymbol{x},t)\boldsymbol{n} = |\nabla\tau|^{-1}\mathrm{div}(\mathring{\boldsymbol{\sigma}}_a(\boldsymbol{x}) + \boldsymbol{p}(\boldsymbol{x})), \quad (3)$$

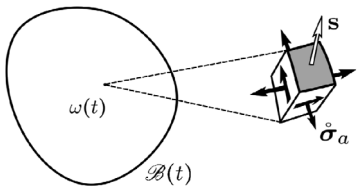


FIG. 1. A sketch of the deposition surface $\omega(t)$ of the body $\mathcal{B}(t)$, showing an infinitesimal element subjected to external tractions $\mathbf{s}$ (three components) and controlled by active surface stresses $\mathring{\boldsymbol{\sigma}}_a$ (three components).

which is the desired boundary condition, first derived apparently in Ref. [27] by a different method, see also Ref. [43].

Next, we assume that inelastic phenomena leading to the accumulation of incompatibilities take place only at the instant of deposition, whereas away from the accreting surface the incremental behavior is linearly elastic. If we neglect the effect of prestress on the incremental behavior [54], we can write $\dot{\boldsymbol{\sigma}} = \mathbb{C}\dot{\boldsymbol{\epsilon}}$, where $\dot{\boldsymbol{\epsilon}} = (\nabla\dot{\boldsymbol{u}} + \nabla\dot{\boldsymbol{u}}^{\mathsf{T}})/2$ and $\dot{\boldsymbol{u}}$ is the incremental displacement. Now, we can solve a sequence of incremental problems and compute the total elastic strain $\boldsymbol{\epsilon}(\boldsymbol{x}, t) = \mathbb{C}^{-1}\boldsymbol{\sigma}(\boldsymbol{x}, t)$, which is generally incompatible.

If we now require that the final incompatibility $\boldsymbol{\eta}(\boldsymbol{x}, t_f) = \mathrm{curlcurl}\boldsymbol{\epsilon}(\boldsymbol{x}, t_f)$ equals its target physiological value $\boldsymbol{\eta}_p(\boldsymbol{x})$, we obtain a constraint on the instantaneous incompatibility of the arriving material $\mathring{\boldsymbol{\eta}} = \mathrm{curlcurl}(\mathbb{C}^{-1}\mathring{\boldsymbol{\sigma}})$ in the form

$$\mathring{\boldsymbol{\eta}} - \nabla\tau \times [\mathrm{curl}\dot{\boldsymbol{\epsilon}}]_{\omega}^{\mathsf{T}} - \mathrm{curl}[\nabla\tau \times \dot{\boldsymbol{\epsilon}}_{\omega}] = \boldsymbol{\eta}_p \quad \text{in} \quad \mathcal{B}(t_f). \tag{4}$$

Here, we used the notation $A_{\omega}(\boldsymbol{x}) \coloneqq A(\boldsymbol{x}, \tau(\boldsymbol{x}))$, see Ref. [43] for details. Since $\dot{\boldsymbol{\epsilon}}(\boldsymbol{x}, t)$ in Eq. (4) implicitly depends on $\mathring{\boldsymbol{\sigma}}_a(\boldsymbol{x})$ through the solution of the incremental problem, we now have a nonlocal relation between the three independent controls of $\mathring{\boldsymbol{\sigma}}_a$ and the three independent targets in $\boldsymbol{\eta}_p$. In the cases when these relations should be understood in the sense of distributions, we implicitly require that in each singular point $\boldsymbol{x}_0$, $\mathbf{B}(\boldsymbol{x}_0, t_f) = \mathbf{B}_p(\boldsymbol{x}_0)$ and $\boldsymbol{\Omega}(\boldsymbol{x}_0, t_f) = \boldsymbol{\Omega}_p(\boldsymbol{x}_0)$. Equation (4), which is the main result of this Letter, defines the deposition strategy that ensures the attainment of a desired stress distribution in physiological conditions.

As an illustration, consider the process of layered manufacturing of an artery [29,31]. For simplicity, the artery will be modeled as a hollow, infinitely long cylinder loaded in plane strain. This is equivalent to replacing a cylinder by a disk which makes the problem two dimensional and fully explicit. We assume that the deposition starts on a rigid mandrel of radius $r_i$ and that the disk grows outwards until the final (physiological) radius $r_f$ is reached. It is convenient to use as a timelike parameter $R = R(t)$, representing the current radius of the accreting surface (line), so that $\tau(R) \equiv R$. Intermediate configurations of the artery are then represented by $r_i \le r \le R \le r_f$. See Fig. 2 for the "macroscopic" rendering of this process: our "microscopic" formulation corresponds to the limit when the thickness of the attached layers $h \to 0$.

If the elastic solid is isotropic and the deposition strategy respects polar symmetry, the incremental displacement reduces to its radial component $\dot{u}(r, R)$. In this case the incremental radial and hoop strains are $\dot{\varepsilon}_r = \partial_r\dot{u}$ and $\dot{\varepsilon}_{\theta} = \dot{u}/r$, respectively, where the superposed dot denotes $\partial/\partial R$. The incremental stress rates $\dot{\sigma}_{r/\theta} = 2\mu\dot{\varepsilon}_{r/\theta} + \lambda(\dot{\varepsilon}_r + \dot{\varepsilon}_{\theta})$,

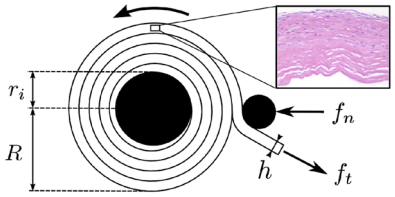


FIG. 2. A sketch of the winding process during artificial manufacturing of an artery, showing the deposition of a layer of thickness $h$ subjected to a passive force $f_n$ and an active force $f_t$. Our microscopic formulation corresponds to the limit $h \to 0$, $f_t \to 0$, while $f_t/h$ remains finite. Inset: the cross section of an artery grown by winding layers of mesenchymal cells (courtesy of Ref. [30]).

where $\lambda$ and $\mu$ are the Lamé moduli, must satisfy the equilibrium equation $\partial_r\dot{\sigma}_r + (\dot{\sigma}_r - \dot{\sigma}_{\theta})/r = 0$.

Observe that the applied tractions have only a radial component $s(R)$, and that the surface component of the deposition stress is fully characterized by its hoop component $\mathring{\sigma}_{a_{\theta}}(R) \sim f_t/h$, see Fig. 2. Then, $(3)_2$ reduces to $\dot{\sigma}_r(R,R) = g(R)$, where $g(R) = s'(R) + [s(R) - \mathring{\sigma}_{a_{\theta}}(R)]/R$. Assuming that displacements are fixed on the rigid mandrel, $\dot{u}(r_i, R) = 0$, we obtain an explicit solution of the incremental problem,

$$\dot{u}(r, R) = \frac{R^2 g(R)}{\mu r_i^2 + (\mu + \lambda)R^2}\frac{r^2 - r_i^2}{2r}. \tag{5}$$

To specify the deposition protocol $\mathring{\sigma}_{a_{\theta}}(r)$ we need to satisfy Eq. (4) and match the target topological constraints imposed through $\mathbf{B}_p$ and $\boldsymbol{\Omega}_p$. In view of our symmetry assumptions, the strain incompatibility tensor reduces to $\boldsymbol{\eta} = \eta(r)\boldsymbol{k} \otimes \boldsymbol{k}$, where the unit vector $\boldsymbol{k}$ is aligned with the cylinder axis, $\eta = \varepsilon_{\theta}'' + (2\varepsilon_{\theta}' - \varepsilon_r')/r$ and $\prime = \partial/\partial r$. Equation (4) reduces to $\mathring{\eta}(R) - [R\dot{\varepsilon}_{\theta}(R,R)]'/R = \eta_p(R)$ and the conditions on a potential line singularity at $r = 0$ take the form $\mathbf{B}_p = \mathbf{0}$ and $\boldsymbol{\Omega}_p = 2\pi\varphi(r_i)r_i\boldsymbol{k}$. Here, we introduce the function $\varphi(r) = \varepsilon_{\theta}' + (\varepsilon_{\theta} - \varepsilon_r)/r$, see Ref. [43] for additional details. Since $\eta = (\varphi r)'/r$, we can recast Eq. (4) in the form $\mathring{\varphi}(R) - \dot{\varepsilon}_{\theta}(R,R) = \varphi_p(R)$, where $\mathring{\varphi}(r)$ refers to the arriving material and $\varphi_p(r)$ to the physiological target state, while $\dot{\varepsilon}_{\theta}(r, R)$ is calculated from Eq. (5). Note that if $\varphi_p(r_i) \neq 0$, the target incompatibility has a nonzero topological (global) component.

If we now assume for determinacy that $s(R) = 0$ and $\mathring{\sigma}_{a_{\theta}}(r_i) = 0$, we can express the function $\mathring{\varphi}(R)$ in terms of $\varphi_p(r)$. This gives the desired deposition strategy securing the attainment of a generic incompatibility:

$$\mathring{\sigma}_{a_{\theta}}(R) = \frac{4\mu(\mu + \lambda)\int_{r_i}^{R}[\mu r_i^2 + (\mu + \lambda)r^2]\varphi_p(r)dr}{(2\mu + \lambda)[\mu r_i^2 + (\mu + \lambda)R^2]}. \tag{6}$$

For arteries, the physiological state is characterized by a finite internal pressure $p$ acting on $r = r_i$ and a much smaller

external pressure acting on $r = r_f$, which we assume to be equal to zero. Under these conditions, stresses in a purely elastic tube would be transmurally inhomogeneous (Fig. 3), which is incompatible with experiments [55] pointing towards homogeneity of the hoop stress [3]. To find the physiologically justified incompatibility that guarantees that $\sigma_\theta^{p\prime} = 0$, we combine this target condition with the equilibrium equation $\sigma_r^{p\prime} + (\sigma_r^p - \sigma_\theta^p)/r = 0$ and obtain that $\sigma_r^p = -p(r_f - r)r_i/[r(r_f - r_i)]$ and $\sigma_\theta^p = pr_i/(r_f - r_i)$. We can now compute the function $\varphi_p(r)$ and substitute it into Eq. (6). The resulting deposition strategy

$$\frac{\mathring{\sigma}_{a_\theta}(R)}{p} = \frac{r_i r_f (R - r_i)[\mu r_i + (\mu + \lambda)R]}{(r_f - r_i)R[\mu r_i^2 + (\mu + \lambda)R^2]} \tag{7}$$

is illustrated in Fig. 3.

Note that the singular component of the incompatibility does not vanish since $\varphi_p(r_i) = p(2\mu + \lambda)r_f/[4\mu(\mu + \lambda)(r_f - r_i)r_i]$; the physiological conditions then require the presence of a "ghost" wedge disclination (or its diffuse analog) aligned with the axis of the artery. Since the nonsingular part of the incompatibility is also different from zero, the residual stresses cannot be relaxed by a single longitudinal cut turning the cylinder into a simply connected domain. This is consistent with experiments on arteries [55], showing that the internal layer (*media*) has a greater opening angle than the external layer (*adventitia*), see the figures in Ref. [43]. Such behavior is also reproduced by our finite element method (FEM) simulations (Fig. 3) for a disk manufactured following the proposed strategy, see Ref. [43] for details on the numerics.

As a second illustration, consider a rather different physiological target that may be relevant for explosive plants [34]. Keeping the same geometry as in the case of arteries, we demand that the distribution of incompatibility is such that the stored elastic energy due to residual stresses is fully released with a single global cut. This requirement will be met if we grow a hollow tube with $\eta_p = 0$ in the bulk and nonzero $\Omega_p$. To this end we must choose $\varphi_p(r) = c/r$, with $c$ a constant characterizing the magnitude of the stored or released energy. The resulting singular incompatibility field can be interpreted as a Volterra wedge disclination with an opening angle $\Omega_p = 2\pi c$ [37,40,43]. If we now substitute this incompatibility into Eq. (6), we obtain that the deposition strategy

$$\frac{\mathring{\sigma}_{a_\theta}(R)}{c} = -\frac{2\mu(\lambda + \mu)}{\lambda + 2\mu}\frac{(\mu + \lambda)(r_i^2 - R^2) + 2r_i^2\mu\log(r_i/R)}{\mu r_i^2 + (\mu + \lambda)R^2}. \tag{8}$$

It is illustrated in Fig. 4, where we also show by FEM simulation that a single longitudinal slicing of a prestressed cylinder with this (purely singular) incompatibility indeed leads to a complete release of the residual stresses, and that subsequent orthogonal slicing does not produce additional relaxation.

To illustrate yet another type of protocols where both tensorial components of the deposition stress, $\boldsymbol{p}(\boldsymbol{x})$ and $\mathring{\boldsymbol{\sigma}}_a(\boldsymbol{x})$, play an active role, we assume that the newly arriving continuum particles are hydrostatically prestressed, with the control parameter $\pi$ representing negative pressure. In the same geometrical setting as above we get $\pi(R) = s(R) = \mathring{\sigma}_{a_\theta}(R)$ and, following an almost identical line of reasoning, we obtain that under such boundary or deposition conditions the strain distribution characterized by a generic function $\varphi_p(R)$ can be reached if we use the protocol

$$\pi(R) = \frac{2(\mu + \lambda)}{r_i^2(2\mu + \lambda)}\int_{r_i}^{R}[\mu r_i^2 + (\mu + \lambda)r^2]\varphi_p(r)dr. \tag{9}$$

Clearly both targets considered above, hoop stress uniformity and a complete release of energy with a single cut,

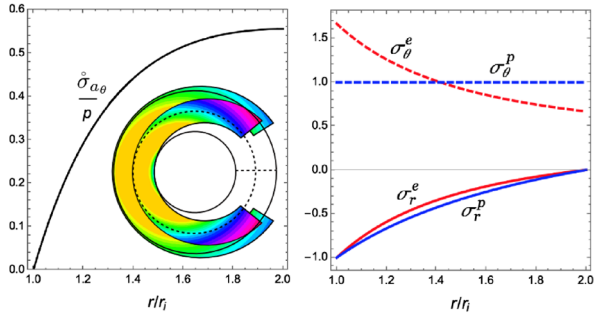


FIG. 3. Left: deposition strategy guaranteeing transmural uniformity of the hoop stress in physiological conditions. The inset shows a FEM simulation illustrating the stress norm (yellow = 0, magenta = max) and the displacement field resulting from cutting the disk along the dashed lines [43]. Right: purely elastic ($\sigma_r^e$, $\sigma_\theta^e$) versus growth induced (inelastic) ($\sigma_r^p$, $\sigma_\theta^p$) stress distributions when an internal pressure $p = 1$.

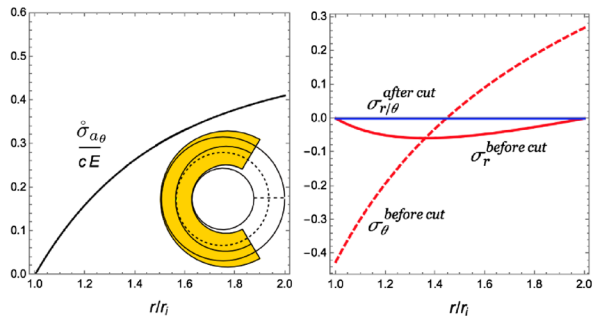


FIG. 4. Left: deposition strategy guaranteeing that the stored elastic energy is completely released by a single cut. The inset shows a FEM simulation of the displacements field resulting from cutting the disk along the dashed lines. The stresses are everywhere zero after the first cut [43]. Right: stresses in the disk before and after the radial cut; $cE = 1$, where $E = 4\mu(\lambda + \mu)/(2\mu + \lambda)$ is the 2D Young modulus.

can be achieved in this framework as well. An important example of such hydrostatic "printing" is crystallisation in a closed container, where the inhomogeneity of the deposition pressure is ensured by the finite compressibility of the melt, e.g., Ref. [49].

In conclusion, we outlined a new theoretical framework for controlled incompatible surface growth and obtained explicit relations that can be used to guide additive manufacturing. Acquiring an ability to generate complex patterns of residual stresses is a crucial step in both biological evolution and the design of biomimetic metamaterials. The proposed surface deposition strategy promises to bring a combination of an unprecedented level of control, together with the ability to handle arbitrarily complex geometries. Future studies are needed to tailor our general theory to specific deposition technologies [56], to extend it to finite strains [57], and to develop an energetic framework coupling the velocity of the accretion front with the corresponding driving forces [58].

The authors thank M. Destrade, P. Recho, and B. Shoikhet for helpful discussions. G. Z. was supported by the ERC Marie Curie Fellowship, INdAM GNFM; L. T. was supported by the French Governement under the Grant No. ANR-10-IDEX-0001-02 PSL.

*giuseppe.zurlo@nuigalway.ie
†lev.truskinovsky@espci.fr

[1] A. S. Gladman, E. A. Matsumoto, R. G. Nuzzo, L. Mahadevan, and J. A. Lewis, Nat. Mater. **15**, 413 (2016).
[2] K. Oliver, A. Seddon, and R. S. Trask, J. Mater. Sci. **51**, 10663 (2016).
[3] C. J. Chuong and Y. C. Fung, J. Biomech. Eng. **108**, 189 (1986).
[4] A. Nilson and D. Darwin, *Design of Concrete Structures* (McGraw-Hill, Inc., New York, 1997), 12 ed., 780 p.
[5] P. J. Withers and H. K. D. H. Bhadeshia, Mater. Sci. Technol. **17**, 366 (2001).
[6] Q. Ge, A. H. Sakhaei, H. Lee, C. K. Dunn, N. X. Fang, and M. L. Dunn, Sci. Rep. **6**, 31110 (2016).
[7] R. Kempaiah and N. Zhihong, J. Mater. Chem. B **2**, 2357 (2014).
[8] J. U. Lind *et al.*, Nat. Mater. **16**, 303 (2017).
[9] A. Geitmann, Cell **166**, 15 (2016).
[10] A. Danescu, C. Chevalier, G. Grenet, Ph. Regreny, X. Letartre, and J. L. Leclercq, Appl. Phys. Lett. **102**, 123111 (2013).
[11] K. Yael, E. Efrati, and E. Sharon, Science **315**, 1116 (2007).
[12] E. Efrati, E. Sharon, and R. J. Kupferman, Mech. Phys. Solids **57**, 762 (2009).
[13] H. Poincaré, *Science and Hypothesis* (The Walter Scott Publishing Co., New York, 1905).
[14] H. Aharoni, J. M. Kolinski, M. Moshe, I. Meirzada, and E. Sharon, Phys. Rev. Lett. **117**, 124101 (2016).
[15] J-H. Na, N. P. Bende, J. Bae, C. D. Santangelo, and R. C. Hayward, Soft Matter **12**, 4985 (2016).
[16] M. Moshe, I. Levin, H. Aharoni, R. Kupferman, and E. Sharon, Proc. Natl. Acad. Sci. U.S.A. **112**, 10873 (2015).
[17] A. Ozakin and A. Yavari, J. Math. Phys. **51**, 032902 (2010).
[18] P. Ciarletta, M. Destrade, and A. L. Gower, Sci. Rep. **6**, 24390 (2016).
[19] R. Skalak, G. Dasgupta, M. Moss, E. Otten, P. Dullemeijer, and H. Vilmann, J. Theor. Biol. **94**, 555 (1982).
[20] R. R. Archer, *Growth Stresses and Strains in Trees* (Springer-Verlag, Berlin, 1986).
[21] D. Correa *et al.*, 3D Printing and Additive Manufacturing **2**, 106 (2015).
[22] I. Gibson, D. Rosen, and B Stucker, *Additive Manufacturing Technologies: 3D Printing, Rapid Prototyping, and Direct Digital Manufacturing* (Springer-Verlag, Berlin, 2014).
[23] N. Kh. Arutyunyan and V. V. Metlov, Mech. of Solids **18**, 140 (1983).
[24] J.-F. Ganghoffer, Int. J. Eng. Sci. **50**, 166 (2012).
[25] P. Ciarletta, L. Preziosi, and G. A. Maugin, JMPS **61**, 852 (2013).
[26] C. B. Brown and L. E. Goodman, Proc. R. Soc. A **276**, 571 (1963).
[27] V. K. Trincher, Izv. AN SSSR. Mekhanika Tverdogo Tela **19**, 119 (1984) [Mech. Solids **19**, 119 (1984)].
[28] A. Bacigalupo and L. Gambarotta, Mech. Based Des. Struc. **40**, 163 (2012).
[29] Y. Jung, H. Ji, Z. Chen, H. Fai Chan, L. Atchison, B. Klitzman, G. Truskey, and K. W. Leong, Sci. Rep. **5**, 15116 (2015).
[30] G. Konig *et al.*, Biomaterials **30**, 1542 (2009).
[31] M. Peck, D. Gebhart, N. Dusserre, T. N. McAllister, and N. L'Heureux, Cells Tissues Organs **195**, 144 (2012).
[32] M. T. Zaucha, R. Gauvin, F. A. Auger, L. Germain, and R. L. Gleason, J. R. Soc., Interface **8**, 244 (2011).
[33] V. D. Varner and C. M. Nelson, Annu. Rev. Chem. Biomol. Eng. **5**, 507 (2014).
[34] H. Hofhuis *et al.*, Cell **166**, 222 (2016).
[35] S. Armon, E. Efrati, R. Kupferman, and E. Sharon, Science **333**, 1726 (2011).
[36] X. Yang, G. Li, T. Cheng, Q. Zhao, C. Ma, T. Xie, T. Li, and W. Yang, J. Appl. Mech. **83**, 071005 (2016).
[37] K-H. Anthony, Arch. Ration. Mech. Anal. **40**, 50 (1971).
[38] M. R. Mitchell, T. Tlusty, and S. Leibler, Proc. Natl. Acad. Sci. U.S.A. **113**, E5847 (2016).
[39] L. Yan, R. Ravasio, C. Brito, and M. Wyart, Proc. Natl. Acad. Sci. U.S.A. **114**, 2526 (2017).
[40] N. Van Goethem and F. Dupret, Eur. J. Appl. Math. **23**, 417 (2012).
[41] V. Volterra, Ann. Sci. Ec. Norm. Super. **24**, 401 (1907).
[42] G. Weingarten, Atti Accad. Lincei Rend. **5**, 57 (1901).
[43] See the Supplemental Material at http://link.aps.org/supplemental/10.1103/PhysRevLett.119.048001, which includes Refs. [44–46], for the derivations of the incremental form of the equilibrium and incompatibility equations, for a discussion of the Burgers and Frank vectors, for details on the numerical calculations carried out in the Letter, and for pictures of arteries manufactured through winding.
[44] A. B. Boley and J. H. Weiner, *Theory of Thermal Stresses* (Dover, New York, 1997).
[45] G. B. Maggiani, R. Scala, and N. Van Goethem, Mathematical Methods in the Applied Sciences **38**, 5217 (2015).

[46] F. J. Hecht, Numer. Math. **20**, 251 (2012).
[47] Since $\mathbf{B}_p$ depends on the choice of the coordinate system, the three degrees of freedom associated with $\mathbf{\Omega}_p \neq 0$ can serve as a complete invariant characterization of the global effect of a defect line.
[48] L. M. Truskinovskiy, Geochem. Int. **21**, 22 (1984) [Geokhimiya **12**, 1744 (1983)].
[49] W. D. King and N. H. Fletcher, J. Phys. D **6**, 21 (1973).
[50] M. A. Holland, T. Kosmata, A. Goriely, and E. Kuhl, Math. Mech. Solids **18**, 561 (2013).
[51] A. V. Manzhirov and S. A. Lychev, Sov. Phys. Dokl. **57**, 160 (2012).
[52] L. Truskinovsky, J. Appl. Math. Mech. (PMM) **51**, 777 (1987).
[53] *Handbuch der Physik III/3*, edited by C. Truesdell, W. Noll, and S. Flugge (Springer, Berlin, 1965).
[54] A. Hoger, J. Elast. **16**, 303 (1986).
[55] G. A. Holzapfel, G. Sommer, M. Auer, P. Regitnig, and R. W. Ogden, Ann. Biomed. Eng. **35**, 530 (2007).
[56] Y. L. Kong, M. K. Gupta, B. N. Johnson, and M. C. McAlpine, Nano Today **11**, 330 (2016).
[57] F. Sozio and A. Yavari, JMPS **98**, 12 (2017).
[58] A. Di Carlo, *Mechanics of Material Forces*, Advances in Mechanics and Mathematics, edited by P. Steinmann and G. A. Maugin (Springer, New York, 2005), Vol. 11, Part III, pp. 53–64.